Available online at www.sciencedirect.com
ScienceDirect
Thin Solid Films 517 (2008) 1086 – 1090
thin solid films
www.elsevier.com/locate/tsf

Influences of silicon nano-crystallized structures on the optical performance of silicon oxynitride rib-type waveguides

Wen-Jen Liu [a,*], Yin-Chieh Lai [b], Min-Hang Weng [c]

[a] Department of Material Science and Engineering, I-Shou University, Kaohsiung, Taiwan, ROC
[b] Institute of Electro-Optical Engineering, National Chiao Tung University, Hsinchu, Taiwan, ROC
[c] National Nano Device Laboratories, Hsin-Shi, Tainan County, Taiwan, ROC

Available online 13 June 2008

Abstract

Silicon oxynitride (SiON) films were deposited on p-type (100) silicon substrates by plasma enhanced chemical vapor deposition (PECVD), at the temperature of 300 °C, using silane (SiH_4), nitrogen (N_2), ammonia (NH_3) and laughing gas (N_2O) as gas precursors. The effects of the processing gas ratio of $N_2O/(N_2+NH_3)$ on the optical properties, microstructure and chemical bonding evolutions of SiON material, and the influences of silicon nano-crystallized structures on the optical performance of SiON-based rib-type optical waveguides were studied. Microstructure evolutions analysis and optical measurements indicated that the refractive index and the extinction coefficient could be precisely determined by controlling the $N_2O/(N_2+NH_3)$ ratio and the thermal annealing process. A greater density and dimension of silicon nano-crystallized structures resulted in more optical scattering effect phenomena occurring between the interface of silicon nano-crystallized structure and SiON matrix and more optical propagation loss.
© 2008 Elsevier B.V. All rights reserved.

Keywords: Waveguide; Silicon oxynitride; PECVD; Optical properties; Optical communication

1. Introduction

In the last few years, following the rapid development of the Internet and multimedia services, the demand for transmission capacity has increased tremendously. This creates a big challenge for the information transmission capacity of the optical fiber network between metropolises and that of the long distance main optical line already set up. Dense wavelength division multiplexing (DWDM) technology is responsible for the original type of transmission capacity variation, and thus enables the capacity of the broadband to increase greatly. Arrayed waveguide grating (AWG) plays a key role in the DWDM system because of its flexibility, low-cost mass production, manufacturing processes similar to VLSI, and ease of integration with other optical electronic ICs.

The optical waveguide can be divided into two main categories in material selection. One is a low index contrast (LIC), such as using silica-based waveguides with a silica cladding [1] and other LIC optical materials [2,3], with low insertion loss performance. However, because of its larger dimension, its application scope is limited. Another is a high index contrast (HIC), such as using silicon waveguides with a silica cladding (silicon-on-insulator, SOI) [4] and other HIC optical materials [5,6]. Silicon oxynitride (SiON), which is considered the candidate material for LIC and HIC optical waveguides, possesses the properties of low residual stress, variations of refractive index controlled by adjusting $N_2O/(N_2+NH_3)$ ratio, and low absorption phenomena for infrared regions [7].

However, the role of Si nano-crystallized structures in SiON film needs to be further clarified. Therefore, the effects of the processing gas ratio of $N_2O/(N_2+NH_3)$ on the optical properties and microstructure evolutions of SiON material, and the influences of silicon nano-crystallized structures on the optical performance of SiON-based, rib-type optical waveguides were investigated.

2. Experimental

2.1. Structure simulation

The schematic structure of a rib-type waveguide was adopted by following Pogossian's single-mode model [8], with indexes

* Corresponding author. Tel.: +886 7 6577262; fax: +886 7 6578444.
E-mail address: jurgen@isu.edu.tw (W.-J. Liu).

0040-6090/$ - see front matter © 2008 Elsevier B.V. All rights reserved.
doi:10.1016/j.tsf.2008.06.021

of 1.50 SiON and 1.45 SiO_2 films as core and top/bottom cladding layers, respectively, as shown in Fig. 1(a). The beam propagation method (BPM), with launch position and optical waveguides length variations for connecting optical fiber and optical waveguides, was studied to achieve reasonable coupling and propagation losses, respectively. Based on the simulation results, the quartz glass masks for AWG devices and straight optical waveguides pattern were designed and manufactured. These straight optical waveguides in the optical mask were used to measure the coupling and propagation losses.

2.2. Fabrication processes

In order to obtain the designed optical properties of SiON film, variations of $N_2O/(N_2+NH_3)$ ratio, in the range of 0.2~ –2.0, were adopted to deposit a 3000 nm thickness of SiO_2 and 6000 nm thickness of SiON single layer films on the D263T quartz glass. The ICP-PECVD system was used, with a radio-frequency (RF) of 13.56 MHz at the substrate temperature of 300 °C with the SiH_4 flow rate of 25 sccm, the NH_3 flow rate of 25 sccm, the N_2 flow rate of 75 sccm, the N_2O flow rate in the range of 20~ –200 sccm, and RF power wattage of 100 W with an operating vacuum pressure of 253 Pa, respectively. The thickness was monitored in-situ by quartz oscillation equipment. The optical transmittances of SiO_2 and SiON single layer films were determined by a Hitachi U-4100 scanning spectrophotometer in the wavelength region of 350–2000 nm. The refractive index and the extinction coefficient were determined by the Swanepoel [9] reported method and obtained a reasonable $N_2O/(N_2+NH_3)$ ratio to fabricate the designed waveguide. Therefore, we used the obtained $N_2O/(N_2+NH_3)$ ratio to deposit a 3000 nm thickness of SiO_2 and 6000 nm thickness of SiON films on the six-inch diameter, p-type (100) silicon wafer, respectively. We then proceeded with the optimum photolithography and reactive etching (C_4F_8/O_2) processes, by using the ICP-RIE system with a radio-frequency of 13.56 MHz at the temperature of 300 °C and using the C_4F_8 flow rate of 45 sccm, the O_2 flow rate in the range of 4–8 sccm, RF power wattage of 2500 W with an operating vacuum pressure of 0.67 Pa, respectively, to investigate the effects of etching reactant ratio (C_4F_8/O_2) on the profile and sidewall roughness of SiON optical waveguides. Subsequently, we annealed the determined etched bi-layer films in a thermal furnace with an oxygen atmosphere at the temperature of 1050 °C and operating pressure of 10,133 Pa for 4 h, respectively, to reduce the N–H bonds of SiON film. We deposited a 3000 nm thickness of SiO_2 to serve as the top cladding for the optical waveguides. Finally, we performed cutting, grinding, and polishing processes to finish the rib-type waveguides, and the optical characteristics of optical straight waveguides were measured by the auto optical coupling stage system, as shown in Fig. 1(b).

Surface roughness of the films was measured below the 5000 nm×5000 nm size by using an atomic force microscope (AFM, Solver Scanning-probe-Microscope SPM-P7LS). Cross-sectional transmission electron microscopy (XTEM) samples were prepared by cutting, mechanical grinding, chemical mechanical polishing, and ion-milling (Gatan Duo-mill) to an electron transparency. High-resolution transmission electron microscopy (HRTEM) was used to observe the cross-sectional microstructure of the SiON core layer, with a JEOL JEM-4000EX type electron microscope operated at a voltage of 400 kV. The density and dimension of silicon nano-crystallized structures in the amorphous SiON optical films were quantitatively calculated with at least 5 TEM images. Optical waveguides profile analysis of the core layer was performed by scanning electron microscopy (SEM, JSM-6400).

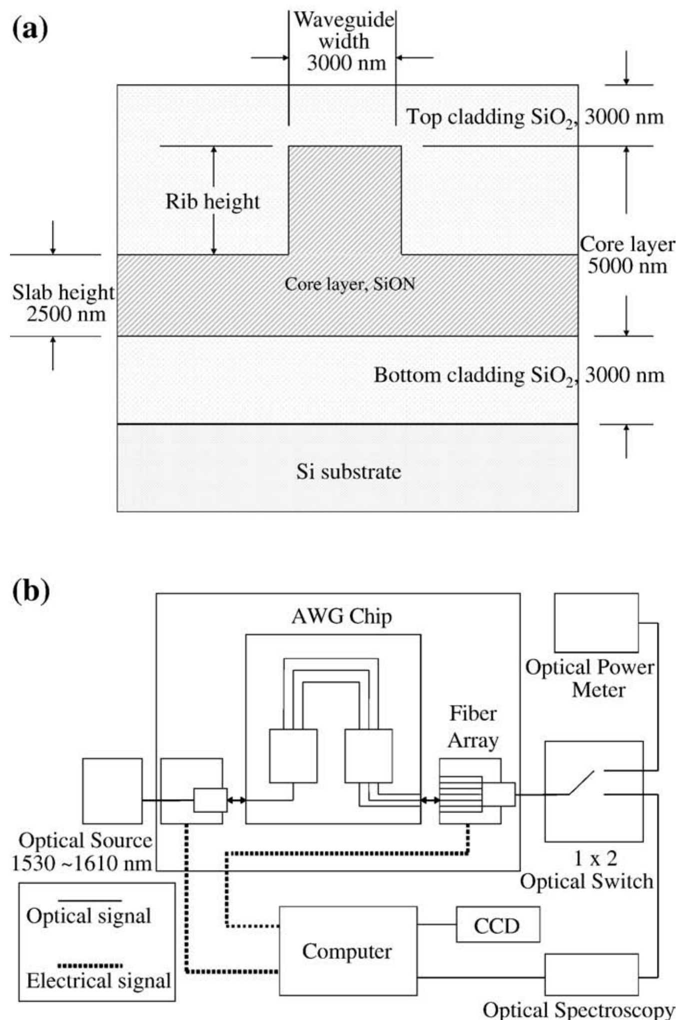

Fig. 1. (a) Schematic structure of small rib-type AWG with an index of 1.50 SiON and an index of 1.45 SiO_2 used as core and top/bottom cladding layers, respectively. (b) Schematic features of auto optical coupling stage system.

3. Results and discussion

3.1. Simulation results

Optical waveguides, with the width of 5000 nm, the height of 6000 nm, the slab height of 4000 nm, and the length of 20 mm, revealed reasonable spectral performance by 3-dimension (3D) simulation, as indicated in Table 1. The waveguide of the smaller dimension, rib-type waveguide design, with an index of

Table 1
Detail simulation parameters for large and small rib-type straight waveguides and AWG with indexes of 1.50 and 1.45 SiON and SiO_2 as core and top/bottom cladding layers, respectively

Items	Large size waveguide	Small size waveguide
Center wavelength	1552.25 nm	1552.25 nm
Output channels	8	8
Optical waveguides structure	Rib	Rib
Optical waveguides height	6000 nm	5000 nm
Optical waveguides width	5000 nm	3000 nm
Slab height	4000 nm	2500 nm
AWG Device dimension	11 cm × 3 cm	4 cm × 1.4 cm
Arrayed optical waveguides numbers	46	36
Center optical waveguides loss (3D)	−0.5 dB	−2.35 dB
Uniformity of loss (3D)	−3.6 dB	−1.9 dB
Center optical waveguides loss (EIM)	−0.05 dB	−0.15 dB
Uniformity of loss (EIM)	−2.9 dB	−1.5 dB
Device crosstalk	<−20 dB	< −15 dB
Device side-lobe	<−35 dB	< −40 dB

1.50 as a core layer, an optical waveguides width of 3000 nm, a height of 5000 nm, a slab height of 2500 nm, and a length of 20 mm, appeared to have better spectral performance and a smaller AWG chip size, as shown in Table 1. The smaller AWG device had the size of 4 cm × 1.4. Therefore, we adopted this smaller dimension, rib-type SiON AWG device and straight optical waveguides for further fabrication.

3.2. Fabrication results

3.2.1. Optical characteristics

The effects of the $N_2O/(N_2+NH_3)$ ratio on the refractive index and extinction coefficient at a center wavelength of 1550 nm, and the deposition rate were shown in Fig. 2. It was found that the refractive index and the extinction coefficient of the SiON films possessed values of 1.45–1.89 and 1×10^{-4}–4.3×10^{-4}, respectively, during different $N_2O/(N_2+NH_3)$ ratios. It is important to accurately select a specified refractive index under a reasonable $N_2O/(N_2+NH_3)$ ratio. When the ratio of $N_2O/(N_2+NH_3)$ is larger than 2.0, the optical characteristics of deposited SiON films became similar to silicon dioxide films (n~1.45), approaching to the conventional silica-based (low index contrast, LIC) rib-type waveguide applications. Oppositely, when the ratio of $N_2O/$(N_2 N_2+NH_3) is smaller than 0.2, the optical characteristics of deposited SiON films became similar to silicon nitride films (n~2.0), approaching to the high index contrast (HIC) rib-type waveguide applications. All LIC and HIC rib-type waveguides materials were initially designed with very low extinction coefficient and propagation loss at 1550 nm wavelength. However, the Si nano-crystallized structures were formed unavoidably under fabrication process in the amorphous SiON films and would result in the high scattering phenomena and increase of the extinction coefficient. So we must consider their negative influences on the rib-type waveguide usage in the future. The SiON films for the $N_2O/(N_2+NH_3)$ ratio at the value of 1.0 when performing the thermal annealing process, indicated no evident variation of the refractive index and the extinction coefficient approached the value of zero. Therefore, the SiON films could achieve the designed refractive index and extinction coefficient by controlling the $N_2O/(N_2+NH_3)$ ratio at the value of 1.0 and performing a thermal annealing process.

3.2.2. Microstructure analysis

It was found that the SiON films possessed a similar amorphous XRD pattern to that of the glass substrate. AFM analysis indicated that the average roughness of the SiON films increased as the $N_2O/(N_2+NH_3)$ ratio value increased, and found that the average roughness values were 0.578 nm, 6.836 nm, and 7.478 nm at the $N_2O/(N_2+NH_3)$ ratios of 0.2, 1.0 and 1.8, respectively. Increasing the $N_2O/(N_2+NH_3)$ ratio, that is, a higher N_2O flow rate, would form a higher density of

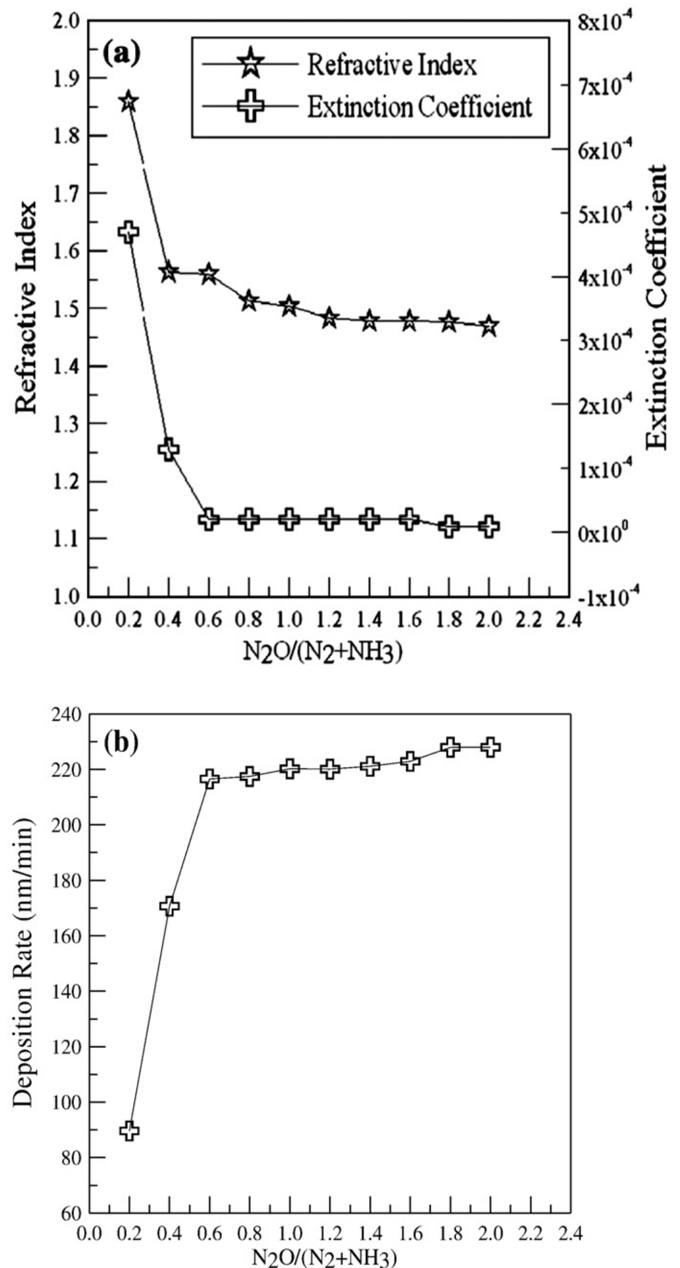

Fig. 2. (a) The refractive index and the extinction coefficient, (b) the deposition rate of SiON film are dependent on the $N_2O/(N_2+NH_3)$ ratio.

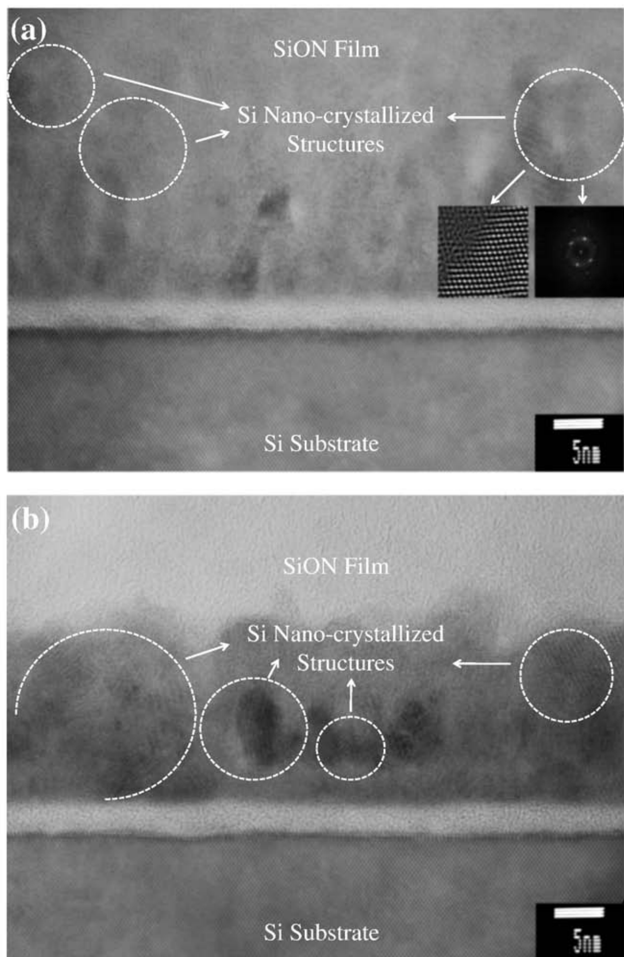

Fig. 3. Transmission electron microscope (TEM) cross-sectional features of the SiON films under the $N_2O/(N_2+NH_3)$ ratios of (a) 0.2 and (b) 1.0.

oxygen free radical atoms than the lower N_2O flow rate, resulting in a larger deposition rate and roughness of SiON film.

TEM analysis was used to observe the localized micro-structure. The cross-sectional features of HRTEM analysis for the SiON films, with $N_2O/(N_2+NH_3)$ ratios of 0.2, and 1.0, respectively, were shown in Fig. 3(a)–(b). TEM examination clearly revealed no evident void formation observed in these un-thermal annealing treated specimens. It was also revealed that on the films there existed few silicon nano-crystallized structures with various dimensions and densities as shown in Table 2. The silicon nano-crystallized structure amounts increased as the $N_2O/(N_2+NH_3)$ ratio decreased, and this resulted in a higher extinction coefficient.

Table 2
XTEM statistical measurement of silicon nano-crystallized structures dimensions and densities

$N_2O/(N_2+NH_3)$ ratio	Dimensions (nm)	Densities ($\times 10^{13}$#/cm^3)
0.2	10–50	~20
1.0	10–30	~3
1.8	<10	~1

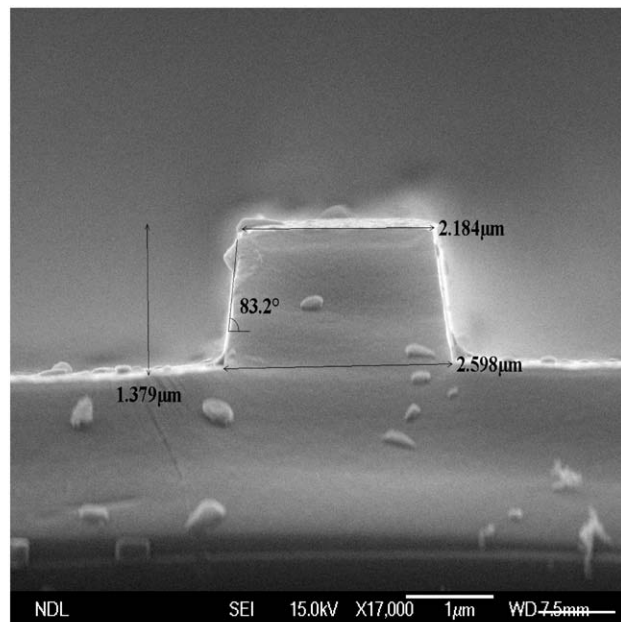

Fig. 4. Optimum cross-sectional etching profile of rib-type SiO_2/SiON films under the C_4F_8/O_2 ratio of 45 sccm/6 sccm.

The substrate holder of the PECVD system is self-biased at the voltage of −200 V by the RF power supply. Si nano-crystallized structures might be nucleated and grown in the vicinity of the defects which are formed by plasma positive ions bombarded the substrate. Moreover, the presence of nitrogen could increase the precipitation density of Si nano-crystallized structures in SiON thin films as in the study of Ehara and Machida [10]. Under the PECVD process, the Si nano-crystallized structures were embedded randomly in the amorphous SiON films by random bombardment of plasma positive ions.

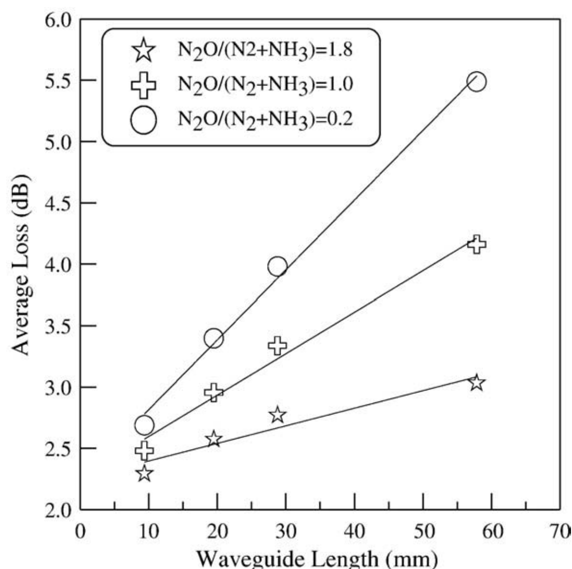

Fig. 5. The coupling loss was about −2.3 dB, and the propagation losses were −0.57 dB/cm, −0.34 dB/cm, and −0.15 dB/cm for the $N_2O/(N_2+NH_3)$ ratios of 0.2, 1.0, and 1.8, respectively.

3.2.3. Etching processes and optical characteristics of waveguides

The topography of rib-type SiO_2/SiON films was influenced by the etching reactant C_4F_8/O_2 ratio of 45 sccm/4 sccm, 45 sccm/6 sccm, and 45 sccm/8 sccm, respectively, and indicated that the optimum vertical etching profile existed at the ratio of 45 sccm/6 sccm, as shown in Fig. 4. It is well-known that the C/F ratio will effectively influence the etching profile for the competition of polymerization and etching processes, and providing sufficient oxygen atoms would evidently reduce the polymerization phenomena [11].

The coupling loss was about −2.23 dB, and the propagation losses were −0.57 dB/cm, −0.34 dB/cm, and −0.15 dB/cm for the $N_2O/(N_2+NH_3)$ ratios of 0.2, 1.0, and 1.8, respectively, as shown in Fig. 5. It was found that the more density and dimension of silicon nano-crystallized structures in the amorphous optical films resulted in more propagation loss, and this might be contributed mainly to a more scattering effect phenomenon which occurred between the interface of silicon nano-crystallized structure and SiON matrix.

4. Conclusion

The refractive index and the extinction coefficient of a SiON film could be precisely determined by controlling the $N_2O/(N_2+NH_3)$ ratio. The silicon nano-crystallized structure amounts would be increased as the $N_2O/(N_2+NH_3)$ ratio decreased, and the more density and dimension of silicon nano-crystallized structures in the amorphous optical films would result in a larger extinction coefficient and more propagation loss. We must consider their unavoidably negative influences on the rib-type waveguide usage in the future.

Acknowledgements

We gratefully acknowledge the support and discussions of the manufacturing process by the National Nano Device Laboratory staff. We also very much appreciate the Next Technologies Co. Ltd. for their assistance in providing the relative optical analysis instruments. This work was financially supported by the National Science Council of the Republic of China under contract number: NSC95-2221-E-214-033.

References

[1] Kazumasa Takada, Makato Abe, IEEE Photonotics Technology. 14 (2002) 813.
[2] Soon Ryong Park, Beom-hoan O, Jaewan Jeong, Seung Gol Lee, El Hang Lee, Optical Materials 21 (2002) 531.
[3] Chun-Sheng Ma, Hai-Ming Zhang, Da-Ming Zhang, Zhan-Chen Cui, Shi-Yong Liu, Optics Communications 241 (2004) 321.
[4] Eric Cassan, Suzanne Laval, Sébastien Lardenois, Alain Koster, IEEE Journal of Selective Topics in Quantum Electron. 9 (2003) 460.
[5] Wen-Jen Liu, Steven Chen, I-Tsen Lai, Hsin-Yen Cheng, Jyung-Dong Lin, Shen-Li Fu, Surface & Coatings Technology 201 (2007) 6581.
[6] Yongjin Wang, Xinli Cheng, Zhilang Lin, Changsheng Zhang, Feng Zhang, Vacuum 72 (2004) 345.
[7] G.-L. Bona, R Germann, BJ Offrein, IBM Journal of Res and Development 47 (2003) 239.
[8] Souren P. Pogossian, Lili Vescan, Adrian Vonsovici, Journal of Lightwave Technology 16 (1998) 1851.
[9] R. Swanepoel, Journal of Physics of the Earth: Science Institution 16 (1983) 1214.
[10] Takashi Ehara, Soushi Machida, Thin Solid Films 346 (1999) 275.
[11] M. Sekine, Applied Surface Science 192 (2002) 270.